HHS Public Access

Author manuscript

Mol Genet Metab. Author manuscript; available in PMC 2018 March 01.

Published in final edited form as:

Mol Genet Metab. 2017 March ; 120(3): 229–234. doi:10.1016/j.ymgme.2017.01.003.

Glycogen storage disease type Ia mice with less than 2% of normal hepatic glucose-6-phosphatase-α activity restored are at risk of developing hepatic tumors

Goo-Young Kim[1], **Young Mok Lee**[1], **Joon Hyun Kwon**[1], **Jun-Ho Cho**[1], **Chi-Jiunn Pan**[1], **Matthew F. Starost**[2], **Brian C. Mansfield**[1,3], and **Janice Y. Chou**[1,*]

[1]Section on Cellular Differentiation, Eunice Kennedy Shriver National Institute of Child Health and Human Development

[2]Division of Veterinary Resources, National Institutes of Health, Bethesda, MD 20892

[3]Foundation Fighting Blindness, Columbia, MD 21046

Abstract

Glycogen storage disease type Ia (GSD-Ia), characterized by impaired glucose homeostasis and chronic risk of hepatocellular adenoma (HCA) and carcinoma (HCC), is caused by a deficiency in glucose-6-phosphatase-α (G6Pase-α or G6PC). We have previously shown that *G6pc*−/− mice receiving gene transfer mediated by rAAV-G6PC, a recombinant adeno-associated virus (rAAV) vector expressing G6Pase-α, and expressing 3–63% of normal hepatic G6Pase-α activity maintain glucose homeostasis and do not develop HCA/HCC. However, the threshold of hepatic G6Pase-α activity required to prevent tumor formation remained unknown. In this study, we constructed rAAV-co-G6PC, a rAAV vector expressing a codon-optimized (co) G6Pase-α and showed that rAAV-co-G6PC was more efficacious than rAAV-G6PC in directing hepatic G6Pase-α expression. Over an 88-week study, we showed that both rAAV-G6PC- and rAAV-co-G6PC-treated *G6pc*−/− mice expressing 3–33% of normal hepatic G6Pase-α activity (AAV mice) maintained glucose homeostasis, lacked HCA/HCC, and were protected against age-related obesity and insulin resistance. Of the eleven rAAV-G6PC/rAAV-co-G6PC-treated *G6pc*−/− mice harboring 0.9–2.4% of normal hepatic G6Pase-α activity (AAV-low mice), 3 expressing 0.9–1.3% of normal hepatic G6Pase-α activity developed HCA/HCC, while 8 did not (AAV-low-NT). Finally, we showed that the AAV-low-NT mice exhibited a phenotype indistinguishable from that of AAV mice expressing ≥ 3% of normal hepatic G6Pase-α activity. The results establish the threshold of hepatic G6Pase-α activity required to prevent HCA/HCC and show that GSD-Ia mice harboring less than 2% of normal hepatic G6Pase-α activity are at risk of tumor development.

*Correspondence should be addressed to: Janice Y. Chou, Building 10, Room 9D42, NIH, 10 Center Drive, Bethesda, MD 20892-1830, Tel: 301-496-1094; Fax: 301-402-6035, chouja@mail.nih.gov.

Conflict of interest

The authors have declared that no conflict of interest exists.

Keywords

Gene therapy; Recombinant adeno-associated virus vector; Hepatocellular adenoma; Hepatocellular carcinoma

1. Introduction

Glycogen storage disease type Ia (GSD-Ia or von Gierke disease, MIM232200) is an autosomal recessive disorder caused by a deficiency in glucose-6-phosphatase-α (G6Pase-α or G6PC) that catalyzes the hydrolysis of glucose-6-phosphate (G6P) to glucose and phosphate in the terminal step of gluconeogenesis and glycogenolysis of the liver, kidney, and intestine [1, 2]. G6Pase-α is a hydrophobic protein anchored in the endoplasmic reticulum by 9 transmembrane helices with its active sites situated inside the lumen [3]. For catalysis, the G6P substrate must be transported from the cytoplasm into the endoplasmic reticulum lumen by a G6P transporter (G6PT), and the G6Pase-α/G6PT complex maintains interprandial blood glucose [1, 2]. Patients affected by GSD-Ia are unable to maintain glucose homeostasis and present with fasting hypoglycemia, hepatomegaly, nephromegaly, hyperlipidemia, hyperuricemia, lactic acidemia, and growth retardation [1, 2]. Untreated, GSD-Ia is juvenile lethal. Dietary therapies [4, 5] have enabled GSD-Ia patients to attain near normal growth and pubertal development. However, no current therapy is able to address the long-term complication of hepatocellular adenoma (HCA) that develops in 75% of GSD-I patients over 25 years-old [1, 2, 6–8]. In 10% cases, HCA undergoes malignant transformation to hepatocellular carcinoma (HCC). In GSD patients classified to date, 52% of HCA are inflammatory HCA, 28% β-catenin mutated HCA and 20% unclassified HCA [9, 10].

We have examined the efficacy of gene therapy mediated by rAAV-G6PC, a recombinant adeno-associated virus (rAAV) pseudotype 2/8 vector expressing human G6Pase-α directed by the human *G6PC* promoter/enhancer (GPE) [11–13]. Systemic administration of rAAV-G6PC delivers the G6Pase-α transgene to the liver of *G6pc*−/− mice and provides a sustained correction of metabolic abnormalities over 90 weeks [12, 13]. The rAAV-G6PC-treated *G6pc*−/− mice expressing 3–63% of normal (or wild-type) hepatic G6Pase-α activity maintain blood glucose homeostasis for 70–90 weeks, show no evidence of HCA/HCC, tolerate a 24-hour fast, and are protected against age-related obesity and insulin resistance [12, 13]. However, the threshold of hepatic G6Pase-α activity required to prevent tumor formation remained unknown. Studies have shown that codon optimization strategies have proven useful to increase translation efficiency [14–17]. We therefore generated a rAAV vector expressing a codon-optimized (co) human G6Pase (co-G6Pase) to determine if this might increase translation efficiency and enzyme activity.

In this study, we examined the efficacy of gene transfer in *G6pc*−/− mice mediated by rAAV-G6PC and rAAV-co-G6PC, and the minimal hepatic G6Pase-α required to prevent tumor formation. We show that the rAAV-co-G6PC vector is more effective than the rAAV-G6PC vector in directing hepatic G6Pase-α expression. All rAAV-G6PC/rAAV-co-G6PC-treated *G6pc*−/− mice expressing 3–33% of normal hepatic G6Pase-α activity (AAV mice) maintain

glucose homeostasis, lack HCA/HCC, and are protected against age-related obesity and insulin resistance. Of the eleven rAAV-treated *G6pc*−/− mice harboring 0.9–2.4% of normal hepatic G6Pase-α activity (AAV-low mice), 3 expressing 0.9–1.3% of normal hepatic G6Pase-α activity (AAV-low-T mice) develop HCA/HCC and 8 did not (AAV-low-NT), showing that mice restoring less than 2% of normal hepatic G6Pase-α activity are at risk of developing hepatic tumors. We also showed that the AAV-low-NT mice exhibited a phenotype indistinguishable from that of AAV mice.

2. Materials and methods

2.1. Construction of pSVL and rAAV vectors and infusion of G6pc−/− mice

The human co-G6PC was synthesized by Life Technologies and subcloned into the pSVL vector, yielding pSVL-co-G6PC. The pTR-GPE-co-G6PC plasmid was constructed by replacing human G6PC at 5′-SbfI and 3′-NotI sites in pTR-GPE-G6PC with the human co-G6PC cDNA. The rAAV vectors were produced at the University of Florida Powell Gene Therapy Center Vector Core Laboratory. All animal studies were conducted under an animal protocol approved by the Eunice Kennedy Shriver National Institute of Child Health and Human Development Animal Care and Use Committee. The rAAV vector was infused into 2-week-old *G6pc*−/− mice as described previously [11–13]. The Age-matched *G6pc*+/+ and *G6pc*+/− mice with indistinguishable phenotype were used as controls. All mice were fed with the standard mouse chow (NIH-31 Open formula mouse/rat sterilizable diet) from ENVIGO (Fredrick, MD, USA). After weaning, the control and rAAV-treated *G6pc*−/− mice were housed separately. The male and female mice were also housed separately with 3 females per cage and 1–3 males per cage. The 3 tumor-bearing mice were housed in 3 different cages.

Hepatic G6Pase-α activity in 66–88-week-old *G6pc*+/+/ *G6pc*+/− mice averaged 171.4 ± 5.7 units, and was designated as the normal value of hepatic G6Pase-α activity. With the exception of the two HCC-bearing mice, mouse liver samples were collected at sacrifice following a 24-hour fast to ensure that hepatic glucose is produced mainly via gluconeogenesis.

2.2. Phosphohydrolase assay

Liver microsome isolation and microsomal G6Pase-α assay were as described previously [11–13]. In phosphohydrolase assays, reaction mixtures (100 μl) containing 50 mM cacodylate buffer, pH 6.5, 10 mM G6P and appropriate amounts of microsomal preparations were incubated at 30 °C for 10 min. Disrupted microsomal membranes were prepared by incubating intact membranes in 0.2% deoxycholate for 20 min at 0 °C. Non-specific phosphatase activity was estimated by pre-incubating disrupted microsomal preparations at pH 5 for 10 min at 37 °C to inactivate the acid-labile G6Pase-α. One unit of G6Pase-α activity represents one nmol G6P hydrolysis per minute per mg microsomal protein. The 60–90 week-old wild-type mice typically averaged 170–180 units G6Pase-α activity in the livers [12, 13].

2.3. Phenotype analysis

Body composition was assessed using the Bruker minispec NMR analyzer (Karlsruhe, Germany). The presence of HCA nodules in mice was confirmed by histological analysis of liver biopsy samples, using 5 or more separate sections per liver. Blood levels of glucose along with hepatic levels of glucose, triglyceride, lactate, and G6P were determined as described previously [12, 13]. Insulin tolerance testing of mice consisted of a 4-hour fast, prior to blood sampling, followed by intraperitoneal injection of insulin at 0.25 IU/kg, and repeated blood sampling via the tail vein for 1 hour [13].

2.4. Quantitative real-time RT-PCR and Western-blot analysis

The mRNA expression was quantified by real-time RT-PCR using the TaqMan probes in an Applied Biosystems QuantStudio 3 Real-Time PCR System (Foster City, CA, USA). Data were normalized to Rpl19 RNA.

2.5. Analysis of ChREBP nuclear localization

The nuclear location of carbohydrate response element binding protein (ChREBP) in mouse liver sections was performed as described previously [13]. Mouse liver paraffin sections (10 μm thickness) were treated with 0.3% hydrogen peroxide in methanol to quench endogenous peroxidases, then blocked with the Avidin/Biotin Blocking Kit (Vector Laboratories, Burlingame, CA, USA). For ChREBP detection, liver sections were incubated serially with a rabbit antibody against ChREBP and a biotinylated anti-rabbit IgG (Vector Laboratories). The resulting complexes were detected with an ABC kit using the DAB Substrate (Vector Laboratories). Sections were counterstained with hematoxylin (Sigma-Aldrich, St Louis, MO, USA) and visualized using a Zeiss Axioskop2 plus microscope equipped with 40X/0.50NA objectives (Carl Zeiss MicroImaging, Jena, Germany). Images were acquired using a Nikon DS-Fil digital camera and NIS-Elements F3.0 imaging software (Nikon, Tokyo, Japan). The percentage of cells in 10 randomly selected fields containing ChREBP positive nuclei was recorded.

2.6. Statistical analysis

The unpaired t test was performed using the GraphPad Prism Program, version 4 (San Diego, CA, USA). Values were considered statistically significant at $p < 0.05$.

3. Results

3.1. Codon-optimized G6Pase-α exhibits increased enzymatic activity

To increase the levels of transgene expression, we constructed a codon-optimized human G6Pase-α construct, co-G6PC. Transient expression in COS-1 cells showed that the pSVL-co-G6PC construct directed 1.8-fold higher G6P hydrolytic activity, compared to the pSVL-G6PC construct (Fig. 1A). We then infused 2-week-old *G6pc−/−* mice with 6×10^{12} viral particles (vp)/kg of rAAV-G6PC or rAAV-co-G6PC vector. At age 12-weeks, hepatic microsomal G6Pase-α activity in rAAV-G6PC- and rAAV-co-G6PC-treated mice were 15% and 32%, respectively of control hepatic G6Pase-α activity (Fig. 1A), confirming that codon optimized rAAV-co-G6PC expresses more hepatic G6Pase-α activity than rAAV-G6PC.

3.2. Minimum hepatic G6Pase-α activity required to prevent HCA/HCC development

Unlike the global G6Pase-α knock-out (*G6pc*−/−) mice [18] that die early before HCA/HCC are expected to develop, the liver-specific *G6pc*-deficient (L-*G6pc*−/−) mice survive to adulthood and all develop HCA by 78 weeks post-gene deletion [19]. We therefore examined the minimum dosage of rAAV vector required to prevent HCA formation in the treated mice. Two-week-old *G6pc*−/− mice were infused with different doses of rAAV-G6PC or rAAV-co-G6PC vectors: 6×10^{12} vp/kg rAAV-G6PC (n = 9, G6PC); 6×10^{12} vp/kg rAAV-co-G6PC (n = 8, co-G6PC), and 2×10^{12} vp/kg rAAV-co-G6PC (n = 9, co-G6PC-low) over an 88-week study.

The mean fasting hepatic G6Pase-α activity of 66–88-week-old control mice was 171.4 ± 5.7 units (normal values of hepatic G6Pase-α activity). In agreement with previous studies using the rAAV-G6PC vector [12, 13], none of the *G6pc*−/− mice receiving gene transfer from either rAAV-G6PC or rAAV-co-G6PC and expressing 3–33% (5–56 units of G6Pase-α activity) of normal hepatic G6Pase-α activity (n = 15, AAV mice) developed HCA/HCC over an 88-week study (Fig. 1B). Eleven rAAV-treated *G6pc*−/− mice expressed 0.9–2.4% (1.5–4.1 units) of normal hepatic G6Pase-α activity (AAV-low mice) and three developed hepatic tumors (Fig. 1B). The two rAAV-G6PC-treated mice with the lowest hepatic G6Pase-α activity of 1.5 units in the non-tumor liver tissues had lesions. One had a small HCA nodule 4.5 mm in diameter, whose size restricted further analysis while the other had a single HCC nodule 24.5 mm in diameter (HCC-1). One AAV-co-G6PC-low-treated mouse with 2.2 units of G6Pase-α activity in the non-tumor liver tissues developed a single HCC lesion of 18 mm in diameter (HCC-2). Interestingly two other mice with similar levels of restored hepatic G6Pase-α activity did not develop HCA/HCC, suggesting that 0.9–1.3% (1.5–2.2 units) of normal hepatic G6Pase-α activity lies at the threshold of HCA/HCC formation (Fig. 1B). While residual G6Pase-α activity in the non-tumor liver tissue of the HCC-bearing mice was detectable, G6Pase-α activity in the HCC lesions was null and non-detectable.

Despite the marked differences in hepatic G6Pase-α activity restored in the rAAV-G6PC-, rAAV-co-G6PC-, or rAAV-co-G6PC-low-treated *G6pc*−/− mice, all treated mice, including the 3 HCA/HCC-bearing mice were leaner and had average body weights (Fig. 1C) and body fat (Fig. 1D) values significantly lower than that of their age-matched control mice. The HCA/HCC-bearing mice (n = 3) exhibited a further reduction in the average body fat values (Fig. 1D). All rAAV-treated *G6pc*−/− mice continued to manifest hepatomegaly and the HCA/HCC-bearing mice exhibited a more pronounced hepatomegaly (Fig. 1E). In summary, none of the AAV mice expressing ≥3% (≥5 units) of normal hepatic G6Pase-α activity developed HCA/HCC. Of the 11 AAV-low mice, 3 developed HCA/HCC (AAV-low-T mice) while 8 did not (AAV-low-NT mice). To simplify discussion, since all AAV and AAV-low-NT mice do not develop tumors (NT) and they exhibited a similar phenotype, they will be classified as AAV-NT mice.

3.3. Phenotype of rAAV-treated mice

The hallmark of GSD-Ia is fasting hypoglycemia [1, 2]. None of the AAV-NT mice suffered hypoglycemia seizures throughout development and their basal blood glucose levels were

similar to that of the control mice (Fig. 2A). The 3 tumor-bearing mice also did not suffer hypoglycemia seizures but their basal blood glucose levels were significantly lower than that of the control and AAV-NT mice (Fig. 2A). Both wild-type and AAV-NT mice could tolerate long fasts (Fig. 2B). The 2 HCC-bearing mice could not tolerate a fast longer than 6 hours. The sole HCA-bearing mouse available for study could tolerate a long fast, but the 24 hour-fasted glucose levels were significant lower than that of wild-type and AAV-NT mice (Fig. 2B). Fasting blood insulin levels in the 66–88-week-old wild-type and AAV-NT mice were 1.23 ± 0.3 and 0.58 ± 0.05 ng/ml, respectively (Fig. 2C). All were within the normal range although insulin levels in the AAV-NT mice were closer to the levels in 10–20 week-old young adult mice than those in their wild-type littermates [20]. Because AAV-NT mice exhibit increased insulin sensitivity, a reduced insulin dose of 0.25 IU/kg was chosen to monitor blood insulin tolerance profiles. While wild-type mice developed age-related insulin resistance, the AAV-NT mice remained insulin sensitive (Fig. 2D), showing that the AAV-NT mice are protected against an age-related insulin resistance. The low blood glucose levels inherent in the tumor-bearing mice prevented us from undertaking an insulin tolerance challenge for these mice.

3.4. Histological and biochemical analysis of the rAAV-treated mice

All AAV-NT mice lacked any notable hepatic histological abnormalities beyond increased glycogen storage (Fig. 3A). The mouse with the small HCA had a well circumscribed lesion with increased glycogen storage in both HCA and non-HCA tissues (Fig. 3A). The HCC-1 and HCC-2 lesions consisted of anisocytotic and anisokaryotic hepatocytes (Fig. 3A). In human GSD-Ia patients with HCA/HCC nodules, there are multiple nodules per liver [9, 10]. In untreated L-*G6pc*−/− mice [19] a similar pattern is seen. Interestingly, the three tumor-bearing AAV-low-T mice only had single lesions in their livers at a similar age, consistent with the restored levels of G6Pase-α activity being borderline for HCA/HCC formation. Because of the low incidence of HCA/HCC in the rAAV-treated GSD-Ia mice and the presence of only a single lesion per mouse, the molecular characterization of the two HCC lesions is very preliminary as described below.

The β-catenin mutated HCA seen in GSD-Ia mice are characterized by high expression of two β-catenin targets glutamate-ammonia ligase (GLUL) and leucine-rich repeat containing G protein-coupled receptor 5 (LGR5) [9]. In contrast, the inflammatory HCA is characterized by a constitutive activation of the signal transducer and activator of transcription 3 (STAT3), a cancer-promoting transcription factor [10]. In the current study, we showed that the levels of mRNA for *Glul and Lgr5* were increased in HCC-1, suggesting that HCC-1 was derived from a β-catenin mutated HCA and the levels of the active p-STAT3-Y705 protein were increased in HCC-2, suggesting that HCC-2 was derived from an inflammatory HCA.

During fasting, blood glucose homeostasis is maintained by endogenous glucose produced in the liver from hydrolysis of G6P by the G6PT/G6Pase-α complex in the terminal step of gluconeogenesis and glycogenolysis [1, 2]. The *G6pc*−/− mice, lacking a functional G6Pase-α, are incapable of producing endogenous glucose in the liver, kidney, or intestine. After 24 hours of fasting, hepatic glucose levels in control and AAV-NT mice were 117.1 ± 6.5 and

60.3 ± 4.2 nmol/mg protein, respectively (Fig. 3B), indicating that sufficient endogenous glucose was produced in the liver that enabled the AAV-NT mice to maintain blood glucose homeostasis during a long fast. While hepatic triglyceride contents in control, AAV-NT, and the 3 tumor-bearing mice were statistically similar, lactate contents were markedly higher in the livers of both AAV-NT and the tumor-bearing mice compared to that of the wild-type mice (Fig. 3C).

3.5. Activation of hepatic ChREBP signaling in AAV-NT mice

Studies have shown that mice over-expressing hepatic ChREBP exhibit improved glucose tolerance compared to controls [21]. We have shown that activation of ChREBP signaling is one pathway that protects the AAV mice from developing age-related insulin resistance [13]. The G6PT-mediated G6P uptake is the rate-limiting step in glucose production by the G6Pase-α/G6PT complex [22] and hepatic G6PT expression and activity were increased in AAV mice [13]. As expected, hepatic *G6pt* transcripts were increased in AAV-NT mice (Fig. 4A). The *G6pt* is a target of Mlx [23] that dimerizes with ChREBP forming the principal transcription factor complex regulating glucose-responsive genes in the liver [24]. The ChREBP signaling can be activated by G6P which promotes ChREBP nuclear translocation [24]. In AAV-NT mice, *Chrebp* transcripts were increased 2-fold, compared to wild-type mice but the *Mix* transcripts were unchanged (Fig. 4A). Hepatic G6P levels were markedly elevated in AAV-NT mice (Fig. 4B). Accordingly, the fractions of nuclear ChREBP protein were increased markedly in AAV-NT livers, compared to controls (Fig. 4C), suggesting that activation of ChREBP-Mlx signaling increased *G6pt* expression.

4. Discussion

GSD-Ia is juvenile lethal unless the loss of blood glucose homeostasis is addressed [1, 2]. While this can be managed with dietary therapies [4, 5], the therapies do not address the serious long-term complication of HCA/HCC with unknown etiology [1, 2, 6–8]. Using rAAV-mediated gene therapy, we have previously shown that rAAV-treated mice reconstituted with 3–63% of normal hepatic G6Pase-α activity (AAV mice) maintain blood glucose homeostasis and do not develop HCA/HCC [12, 13]. We further showed that the AAV mice are protected against age-related obesity and insulin resistance, and that activation of hepatic ChREBP signaling is one mechanism responsible for the beneficial metabolic phenotype of the mice [13]. We now show that rAAV-G6PC- and rAAV-co-G6PC-treated *G6pc*−/− mice expressing 3–33% of normal (averaged 171.4 ± 5.7 units) hepatic G6Pase-α activity (AAV mice) also maintained glucose homeostasis, lacked HCA/HCC, and were protected against age-related obesity and insulin resistance. We further show that 3 AAV-low-T mice expressing 0.9–1.3% (1.5–2.2 units) of normal hepatic G6Pase-α activity develop hepatic tumors, establishing that *G6pc*−/− mice expressing less than 2% of normal hepatic G6Pase-α activity are at risk of development HCA/HCC. Finally, we show the non-tumor-bearing AAV-low-NT mice expressing 0.9–2.4% (1.5–4.1 units) of normal hepatic G6Pase-α activity display a phenotype indistinguishable from that of the AAV mice with ≥3% of normal hepatic G6Pase-α activity.

To translate rAAV-mediated gene therapy in murine GSD-Ia to the clinic, the safety concerns associated with administering the vector must be addressed. One approach to maintaining therapeutic benefit, while reducing potential toxicities and immune activation associated with *in vivo* administration is to reduce the dose by increasing the potency of the gene transfer vectors. We therefore generated a codon-optimized human G6Pase-α construct and showed that the rAAV-co-G6PC vector was 2-fold more active than the rAAV-G6PC vector in directing hepatic G6Pase-α expression.

Interprandial glucose homeostasis is maintained by the G6PT/G6Pase-α complex and the rate-limiting step is G6PT-mediated G6P uptake [1, 2]. We have shown that reduction of hepatic G6Pase-α expression is accompanied by a compensating stimulation of *G6pt* expression, enabling AAV mice expressing as little as 5 units of hepatic G6Pase-α activity to maintain glucose homeostasis [12, 13]. In human GSD-Ia patients [9] and L-*G6pc*−/− mice [19], who do develop HCA/HCC, there are many lesions co-existing in the same liver. In contrast, when *G6pc*−/− mice are treated with rAAV-mediated G6Pase-α gene therapy, the few mice that do develop lesions, only have a single lesion. Since G6Pase-α activity is restored unevenly throughout the liver with numerous foci containing markedly higher levels of enzymatic activity than the surrounding hepatic tissue [12], this would suggest that even a minimal restoration of G6Pase-α activity in a hepatocyte may reduce the severity of HCA/HCC. Hepatocytes harboring 0.9–1.3% (1.5–2.2 units) of normal hepatic G6Pase-α activity appear to be at risk of HCA/HCC development. We have previously shown that six rAAV-G6PC-treated *G6pc*−/− mice expressing 1–2.2 units of hepatic G6Pase-α activity did not develop hepatic tumors [25]. Therefore, the actual threshold and confirmation of the pathways is limited by the low incidence of lesions and the challenge of finely tuning very low levels of reconstituted G6Pase-α activity.

One potential concern is that dietary competition could lead to differences in dietary compliance for the rAAV-treated mice, and dietary competition, especially between genders in the treated mice, could confound results. Therefore in this study, the rAAV-treated and control mice were housed separately and moreover within the rAAV-treated and control groups the male and female mice were housed separately. Therefore, the likelihood of food access as an additional risk factor for liver tumor development was minimized. To date, we have examined tumor development in 55 rAAV-treated *G6pc*−/− mice that lived to 66–90 week-old and expressed 0.9–63% of normal hepatic G6Pase-α activity, including 17 mice expressing 0.9–2.4% of normal hepatic G6Pase-α activity [12, 13, 25, this study]. Among the 17 mice expressing 0.9–2.4% of normal hepatic G6Pase-α activity [25, this study], three mice developed HCA/HCC. Therefore, the incidence of tumor development in rAAV-treated *G6pc*−/− mice is low which correlates with levels of normal hepatic G6Pase-α activity restored.

In summary, we showed that AAV mice expressing ≥ 3% (5 units) of normal hepatic G6Pase-α activity maintain blood glucose homeostasis, do not develop HCA/HCC, and are protected against age-related obesity and insulin resistance. We further showed that AAV-low-NT mice expressing 0.9–2.4% of normal hepatic G6Pase-α activity exhibited a phenotype indistinguishable from that of AAV mice. Finally, we showed that hepatocytes

harboring less than 2% of normal hepatic G6Pase-α activity are at risk of malignant transformation.

Acknowledgments

We thank Dr. Thomas J. Conlon for helpful discussions of codon optimization methods. This research was supported by the Intramural Research Program of the Eunice Kennedy Shriver National Institute of Child Health and Human Development, National Institutes of Health, and The Children's Fund for Glycogen Storage Disease Research.

Abbreviations

AAV	adeno-associated virus
ChREBP	carbohydrate response element binding protein
G6Pase-α	glucose-6-phosphatase-α
G6P	glucose-6-phosphate
G6PT	glucose-6-phosphate transporter
GPE	*G6PC* promoter and enhancer
GSD-Ia	glycogen storage disease type Ia
HCA	hepatocellular adenoma
HCC	hepatocellular carcinoma

References

1. Chou JY, Matern D, Mansfield BC, Chen YT. Type I glycogen storage diseases: disorders of the glucose-6-phosphatase complex. Curr Mol Med. 2002; 2:121–143. [PubMed: 11949931]
2. Chou JY, Jun HS, Mansfield BC. Glycogen storage disease type I and G6Pase-β deficiency: etiology and therapy. Nat Rev Endocrinol. 2010; 6:676–688. [PubMed: 20975743]
3. Pan CJ, Lei KJ, Annabi B, Hemrika W, Chou JY. Transmembrane topology of glucose-6-phosphatase. J Biol Chem. 1998; 273:6144–6148. [PubMed: 9497333]
4. Greene HL, Slonim AE, O'Neill JA Jr, Burr IM. Continuous nocturnal intragastric feeding for management of type 1 glycogen-storage disease. N Engl J Med. 1976; 294:423–425. [PubMed: 813144]
5. Chen YT, Cornblath M, Sidbury JB. Cornstarch therapy in type I glycogen storage disease. N Engl J Med. 1984; 310:171–175. [PubMed: 6581385]
6. Labrune P, Trioche P, Duvaltier I, Chevalier P, Odievre M. Hepatocellular adenomas in glycogen storage disease type I and III: a series of 43 patients and review of the literature. J Pediatr Gastroenterol Nutr. 1997; 24:276–279. [PubMed: 9138172]
7. Rake JP, Visser G, Labrune P, Leonard JV, Ullrich K, Smit GP. Glycogen storage disease type I: diagnosis, management, clinical course and outcome. Results of the European Study on Glycogen Storage Disease Type I (ESGSD I). Eur J Pediatr. 2002; 161(Suppl 1):S20–34. [PubMed: 12373567]
8. Franco LM, Krishnamurthy V, Bali D, Weinstein DA, Arn P, Clary B, Boney A, Sullivan J, Frush DP, Chen YT, Kishnani PS. Hepatocellular carcinoma in glycogen storage disease type Ia: a case series. J Inherit Metab Dis. 2005; 28:153–162. [PubMed: 15877204]
9. Calderaro J, Labrune P, Morcrette G, Rebouissou S, Franco D, Prévot S, Quaglia A, Bedoss P, Libbrecht L, Terracciano L, Smit GP, Bioulac-Sage P, Zucman-Rossi J. Molecular characterization

of hepatocellular adenomas developed in patients with glycogen storage disease type I. J Hepatol. 20133; 58:50–357.

10. Pilati C, Zucman-Rossi J. Mutations leading to constitutive active gp130/JAK1/STAT3 pathway. Cytokine Growth Factor Rev. 2015; 26:499–506. [PubMed: 26188635]
11. Yiu WH, Lee YM, Peng WT, Pan CJ, Mead PA, Mansfield BC, Chou JY. Complete normalization of hepatic G6PC deficiency in murine glycogen storage disease type Ia using gene therapy. Mol Ther. 2010; 18:1076–1084. [PubMed: 20389290]
12. Lee YM, Jun HS, Pan CJ, Lin SR, Wilson LH, Mansfield BC, Chou JY. Prevention of hepatocellular adenoma and correction of metabolic abnormalities in murine glycogen storage disease type Ia by gene therapy, Hepatology. 2012; 56:1719–1729.
13. Kim GY, Lee YM, Cho JH, Pan CJ, Jun HS, Springer DA, Mansfield BC, Chou JY. Mice expressing reduced levels of hepatic glucose-6-phosphatase-alpha activity do not develop age-related insulin resistance or obesity. Hum Mol Genet. 2015; 24:5115–5125. [PubMed: 26089201]
14. Sharp PM, Li WH. The codon Adaptation Index-a measure of directional synonymous codon usage bias, and its potential applications. Nucleic Acids Res. 1987; 15:1281–1295. [PubMed: 3547335]
15. Foster H, Sharp PS, Athanasopoulos T, Trollet C, Graham IR, Foster K, Wells DJ, Dickson G. Codon and mRNA sequence optimization of microdystrophin transgenes improves expression and physiological outcome in dystrophic mdx mice following AAV2/8 gene transfer. Mol Ther. 2008; 16:1825–1832. [PubMed: 18766174]
16. Ward NJ, Buckley SM, Waddington SN, Vandendriessche T, Chuah MK, Nathwani AC, McIntosh J, Tuddenham EG, Kinnon C, Thrasher AJ, McVey JH. Codon optimization of human factor VIII cDNAs leads to high-level expression. Blood. 2011; 117:798–807. [PubMed: 21041718]
17. Qian W, Yang JR, Pearson NM, Maclean C, Zhang J. Balanced codon usage optimizes eukaryotic translational efficiency. PLoS Genet. 2012; 8:e1002603. [PubMed: 22479199]
18. Lei KJ, Chen H, Pan CJ, Ward JM, Mosinger B, Lee EJ, Westphal H, Mansfield BC, Chou JY. Glucose-6-phosphatase dependent substrate transport in the glycogen storage disease type 1a mouse. Nat Genet. 1996; 13:203–209. [PubMed: 8640227]
19. Mutel E, Abdul-Wahed A, Ramamonjisoa N, Stefanutti A, Houberdon I, Cavassila S, Pilleul F, Beuf O, Gautier-Stein A, Penhoat A, Mithieux G, Rajas F. Targeted deletion of liver glucose-6 phosphatase mimics glycogen storage disease type 1a including development of multiple adenomas. J Hepatol. 2011; 54:529–537. [PubMed: 21109326]
20. Flatt PR, Bailey CJ. Development of glucose intolerance and impaired plasma insulin response to glucose in obese hyperglycaemic (ob/ob) mice. Horm Metab Res. 1981; 13:556–560. [PubMed: 7028589]
21. Benhamed F, Denechaud PD, Lemoine M, Robichon C, Moldes M, Bertrand-Michel J, Ratziu V, Serfaty L, Housset C, Capeau J, Girard J, Guillou H, Postic C. The lipogenic transcription factor ChREBP dissociates hepatic steatosis from insulin resistance in mice and humans. J Clin Invest. 2012; 122:2176–2194. [PubMed: 22546860]
22. Arion WJ, Lange AJ, Ballas LM. Quantitative aspects of relationship between glucose 6-phosphate transport and hydrolysis for liver microsomal glucose-6-phosphatase system. Selective thermal inactivation of catalytic component in situ at acid pH. J Biol Chem. 1976; 251:6784–6790. [PubMed: 10305]
23. Ma L, Robinson LN, Towle HC. ChREBP*Mlx is the principal mediator of glucose-induced gene expression in the liver. J Biol Chem. 2006; 281:28721–28730. [PubMed: 16885160]
24. Filhoulaud G, Guilmeau S, Dentin R, Girard J, Postic C. Novel insights into ChREBP regulation and function, Trends Endocrinol. Metab. 2013; 24:257–268.
25. Lee YM, Kim GY, Pan CJ, Mansfield BC, Chou JY. Minimal hepatic glucose-6-phosphatase-alpha activity required to sustain survival and prevent hepatocellular adenoma formation in murine glycogen storage disease type Ia, Mol. Genet Metab Rep. 2015; 3:28–32.

Highlights

- Confirm that restoring ≥ 3% of normal hepatic G6Pase-α activity fully prevent the development of HCA/HCC in murine GSD-Ia
- Establish that GSD-Ia mice with hepatocytes harboring 0.9–1.3% of normal hepatic G6Pase-α activity are at risk of developing HCA/HCC
- Show that non-tumor-bearing GSD-Ia mice harboring 0.9–33% of normal hepatic G6Pase-α activity are protected against age-related obesity and insulin resistance

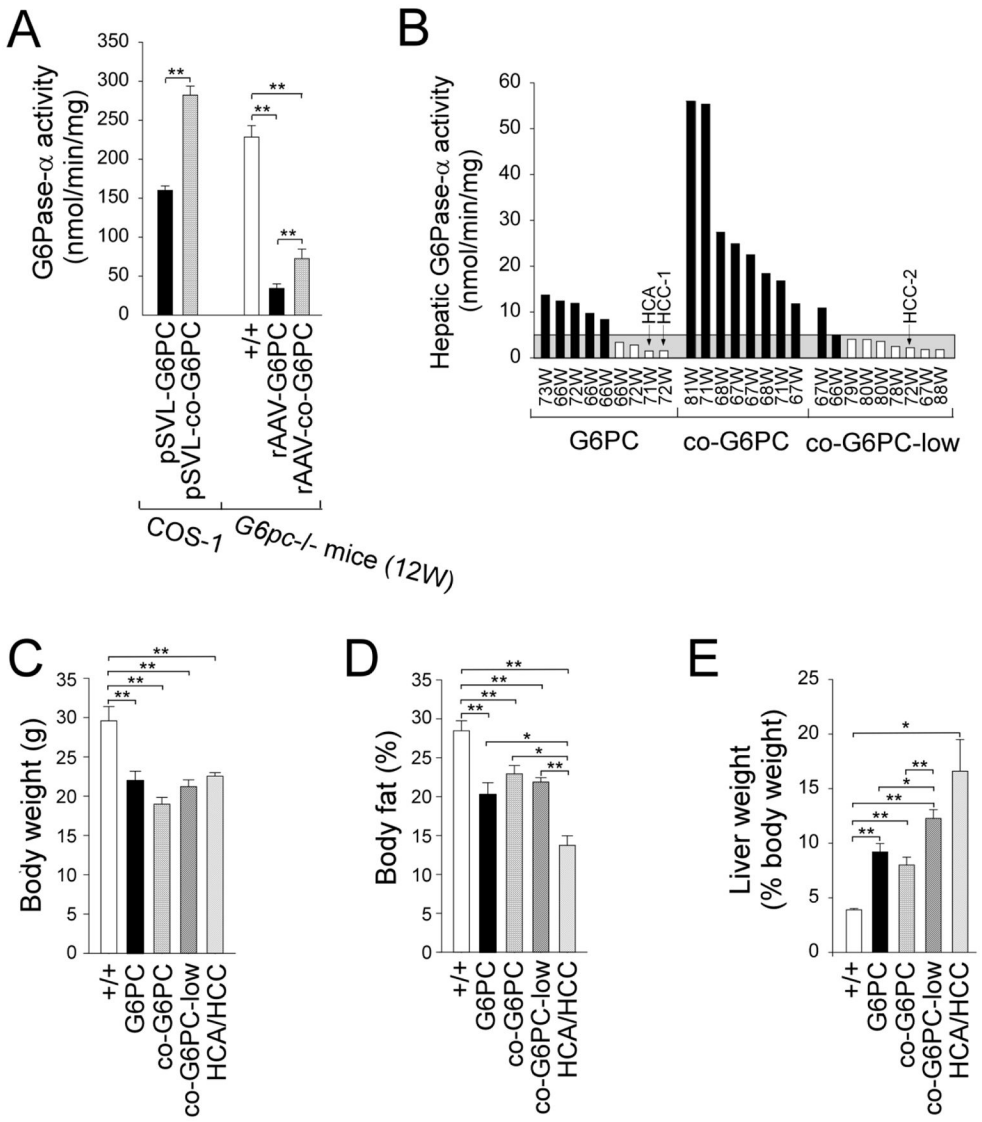

Fig. 1.

Functional characterization of G6PC and co-G6PC constructs and phenotype analysis of rAAV-treated *G6pc*−/− mice. (A) Analysis of G6PC and co-G6PC constructs by transient expression and gene transfer into *G6pc*−/− mice. Transient expression assays were performed in COS-1 cells using two independent pSVL-G6PC or pSVL-co-G6PC isolates, each in four separate transfections. *In vivo* gene delivery was performed by infusing 2-week-old *G6pc*−/− with 6×10^{12} vp/kg of rAAV-G6PC (n = 4) or rAAV-co-G6PC (n = 4), and hepatic G6Pase-α activity was analyzed at age 12 weeks. +/+, wild-type mice. (B–E) Phenotypic analysis of 66–88 week-old wild-type and rAAV-treated *G6pc*−/− mice. Two-week-old *G6pc*−/− were infused with 6×10^{12} vp/kg of rAAV-G6PC (G6PC; n = 9), 6×10^{12} vp/kg of rAAV-co-G6PC (co-G6PC; n = 8), or 2×10^{12} vp/kg of rAAV-co-G6PC (co-G6PC-low; n = 9) and phenotyped at age 66–88 weeks. (B) Hepatic microsomal G6Pase-α activity is shown at the indicated ages in weeks (W). Hepatic G6Pase-α activity in age-matched wild-type mice (+/+, n = 23) averaged 171.4 ± 5.7 units. The grey area denotes

G6Pase activity of ≤5 units. Mice with G6Pase activities ≥ 5 units and <5 units were shown in black and white bars, respectively. (C–E) Body weight (C), body fat (D), and liver weight (E) values in wild-type (+/+, n = 12), rAAV-G6PC (n = 7), rAAV-co-G6PC (n = 8), rAAV-co-G6PC-low (n = 8), and HCA/HCC-bearing (n = 3) mice.

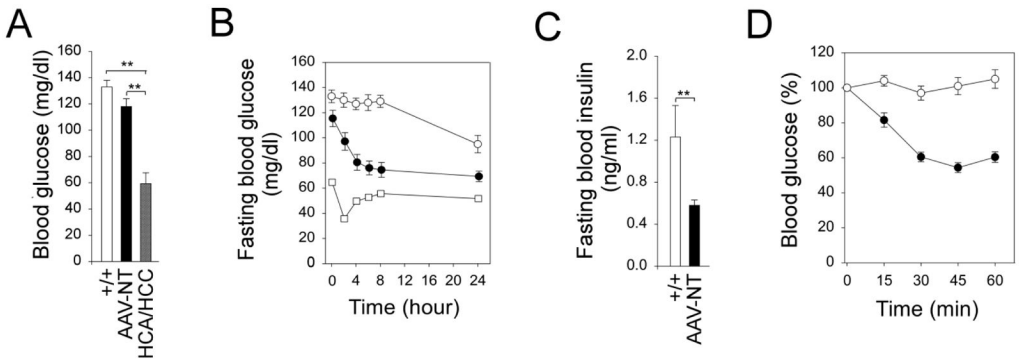

Fig. 2.

Phenotype, fasting blood glucose profile and insulin tolerance profile of 66–88 week-old wild-type and rAAV-treated *G6pc*−/− mice. (A) Blood glucose levels in wild-type (+/+, n = 12), AAV-NT (n = 22), and HCA/HCC-bearing (n = 3) mice. (B) Fasting blood glucose profiles in wild-type (○, n = 12), AAV-NT (●, n = 20) mice, and a single HCA-bearing mouse (□). (C) Twenty-four hour fasted blood insulin levels in wild-type (+/+, n = 12) and AAV-NT (n = 22) mice. (D) Insulin tolerance profiles of wild-type (○, n = 12) and AAV-NT (●, n = 20) mice. Values are reported as a percent of respective level of each group at zero time. Data represent the mean ± SEM; $^{**}P < 0.005$.

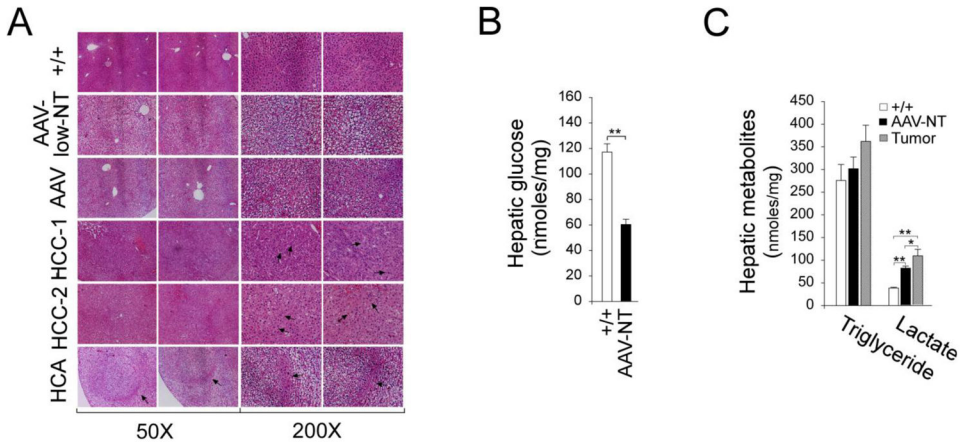

Fig. 3.

Histological analysis and hepatic metabolites in 66–88 week-old wild-type, rAAV-treated *G6pc*−/− mice, and HCA/HCC lesions. The data were analyzed for wild-type (+/+, n = 12), AAV-NT (n = 22), and the single HCA-bearing mice after 24 hours of fasting. The 2 HCC-bearing mice did not undergo fasting. (A) H&E stained liver sections. In HCA-bearing liver, the HCA lesion is denoted by arrows. In HCC-1 and HCC-2, arrows denote anisocytotic and anisokaryotic hepatocytes. Scale bar: 200 μm. (B) Hepatic glucose levels. (C) Hepatic triglyceride and lactate levels. Data represent the mean ± SEM; $^{**}P < 0.005$.

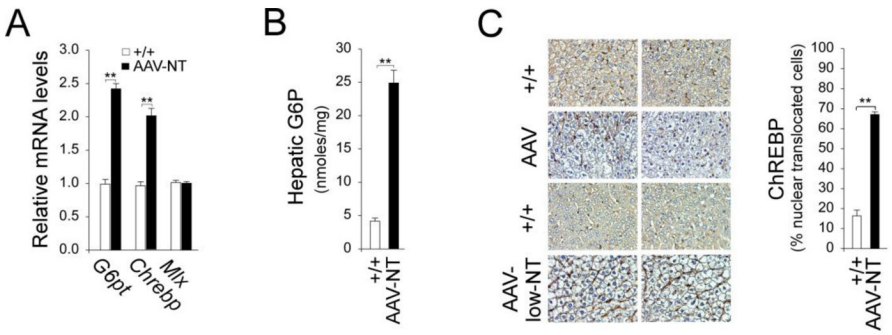

Fig. 4.

Hepatic ChREBP signaling in 66–88 week-old rAAV-treated *G6pc*−/− mice. For hepatic G6P and quantitative RT-PCR, the data were analyzed for wild-type (+/+, n = 12) and AAV-NT (n = 22) mice after 24 hours of fasting. (A) Quantification of *G6pt*, *Chrebp* and *Mlx* mRNA by real-time RT-PCR. (B) Hepatic G6P contents. (C) Immunohistochemical analysis of hepatic ChREBP nuclear localization and quantification of nuclear ChREBP-translocated cells. Representative plates shown are at magnifications of x400, analyzed in wild-type (+/+, n = 5), AAV-NT, including AAV (n = 6), and AAV-low-NT (n = 6) mice. Data represent the mean ± SEM; $^{**}P < 0.005$.